Journal of Molecular Liquids 155 (2010) 71–79

Contents lists available at ScienceDirect

Journal of Molecular Liquids

journal homepage: www.elsevier.com/locate/molliq

NMR relaxation evidence for solute-induced nanosized superstructures in ultramolecular aqueous dilutions of silica–lactose

Jean-Louis Demangeat *

Nuclear Medicine Department, General Hospital, Haguenau, France

ARTICLE INFO

Article history:
Received 3 March 2010
Received in revised form 6 May 2010
Accepted 13 May 2010
Available online 21 May 2010

Keywords:
Proton NMR relaxation
Water
Ultrahigh dilution
Silica

ABSTRACT

We investigated 20 MHz water proton NMR longitudinal (T1) and transverse (T2) relaxation in ultrahigh dilutions (range 10^{-7} M–10^{-47} M) of a mixture of silica–lactose (Sil/Lac) in various media (water, 0.15 M NaCl, 0.15 M LiCl) and in various containers (glass, polyethylene). The samples were prepared by iterative centesimal dilutions under vigorous agitation and rigorously controlled laboratory conditions. Water and salt media were similarly and simultaneously treated, as controls. No significant effect on relaxation times was induced by the iterative dilution/agitation process in pure water and salt controls. By contrast, a slight increase in T1 and decrease in T2 was observed with increasing dilution in silica–lactose solutions, resulting in a marked progressive increase in T1/T2, especially in LiCl medium, distinguishable up to the ultrahigh dilution level. Cross-correlation analyses between T1, T2 and T1/T2 managed to demonstrate opposite behaviours of controls and Sil/Lac dilutions, even in the ultramolecular range of dilution. The effect seemed dependent on the medium (LiCl>NaCl>Water), and was observed in the glassware and polyethylene series as well. After a heating/cooling cycle directly in the sealed NMR tubes, the relaxation variations observed as a function of dilution totally vanished, and the T1/T2 ratio dropped, indicating a less ordered structure. These findings were interpreted in terms of nanosized superstructures with motional correlation time greater than 5.10^{-9} s, nucleated around the solute, and composed of water, ions and nanobubbles generated during the vigorous mechanical process. Incidentally, a striking catalytic enhancement of silica leaching was observed during the preparation of silica–lactose dilutions in glassware; but this did not influence the NMR relaxation results.

1. Introduction

Despite positive meta-analyses of hundreds of studies [1–4], the clinical efficiency of ultrahighly diluted substances, as used in the homeopathic practice, remains controversial [5,6]. According to the pharmacopoeia, homeopathic remedies are prepared following a specific iterative centesimal dilution procedure under vigorous agitation, named dynamization (C1 corresponding to a 10^2-fold dilution, and Cn to a 10^{2n}-fold dilution), so that the solute concentration rapidly reaches the theoretical limit of molecular presence, around C12; which is the stumbling block. In the world of experimental biology, a fierce controversy broke out in 1988 when Benveniste's team reported that ultrahighly diluted antiserum against IgE (up to C60, i.e. well beyond the Avogadro limit) could induce the degranulation of sensitized basophils [7–10]. According to Benveniste, the bio-information should lie in the solvent (the so-called "Memory of water"). His subsequent experiments, which aimed at explaining the claimed effect, supported evidence that electromagnetic signals (EMS) are emitted from the solution, which may be directly transduced to the solvent or recorded, digitized and transmitted to pure water or cells (neutrophils) by means of an electronic device, to produce specific biological effects [11–13]. Similar attempts at demonstrating non-molecular information transfer were carried out by other teams with positive [14,15] and negative [16] results. It is noteworthy that the French virologist Nobel prize-winning Montagnier recently reported a series of experiments showing, by means of the electronic device previously designed by Benveniste, that some bacterial DNA sequences are able to induce distinct EMS as a function of high dilutions ranging from 10^{-5} to 10^{-12} (up to 10^{-18} in one experiment), provided that the dilutions had previously been submitted to a strong agitation [17]. Moreover, he showed that the signal-emitting structures could be transferred from tube to tube by using wave transfer, corroborating the above-mentioned experiments. These EMS were not observed in the first dilutions and were destroyed by heating or freezing the samples. The researcher proposed that polymeric nanostructures form in the samples during the dilution process. This paper will focus on such a hypothesis.

For nearly 20 years we have been studying by nuclear magnetic resonance (NMR) ultrahighly diluted aqueous dilutions and managed to show solute-induced modifications in the water proton relaxation,

* Nuclear Medicine Department, General Hospital, PO Box 40252, F-67504 Haguenau Cedex, France
E-mail address: jean-louis.demangeat@ch-haguenau.fr.

0167-7322/$ – see front matter © 2010 Elsevier B.V. All rights reserved.
doi:10.1016/j.molliq.2010.05.010

distinguishable up to the C12–C21/C24 ultramolecular range of dilution [18–21]. These physical modifications have been reproduced with various solvents (water, saline), various solutes (mixture silica–lactose, manganese, histamine) and various NMR devices (Bruker Minispec at 4 and 20 MHz, IBM field-cycling relaxometer (NMRD) working in the 0.02–4 MHz frequency range). They were more pronounced in saline (0.15 M NaCl) than in water and were destroyed by heating, what led us to propose the presence of nanosized (about 4-nm) superstructures in dilutions, involving water molecules, ions and nanobubbles of dissolved atmospheric gases, nucleated around the solute [21]. However, we could not *a priori* rule out artefacts due to contaminating leached silica (known to promote polymolecular edifices [22]) since all samples were prepared in glass vessels; indeed, we found in the NMRD study on silica–lactose higher amounts of leached silica than expected, especially in the most highly diluted samples [20]. Therefore, the present study has been designed to replicate at 20 MHz the results obtained in the 0.02–4 MHz NMRD study, and to focus on the role of leached silica and of the ionic medium, by preparing a set of samples in polyethylene vessel with 0.15 M lithium chloride as solvent. The previously described physical modifications in high dilutions compared to solvents will be reproduced, especially in samples prepared in plastic ware, where they appear to be even more pronounced, due to the LiCl medium.

2. Experimental

2.1. Preparation of samples

The preparation of the samples was carried out under controlled atmospheric conditions following a specific iterative centesimal dilution procedure, through vigorous agitation achieved either by a Cenco vortex (20 s at maximal rate) or by a specific mechanical apparatus manufactured by Boiron (vertical stroker) for industrial applications which produces 300 violent vertical strokes in 14 s. As controls, the solvents were submitted to strictly identical dilution/agitation procedures. All solutions and similarly treated solvents belonging to one series were prepared within half a day, in order to avoid barometric and temperature fluctuations. Five to six independent series were prepared per experimental set, at intervals of about one month. For each series, new batches of solvents were used and the order in which the solutions and solvents were prepared was randomly permuted. All operations were carried out under a laminar-flow exhaust hood in sterile conditions, with fresh material, including vials, glass droppers, caps and NMR tubes, previously cleaned with 70% alcohol of spectroscopic quality and three times rinsed with bidistilled water before sterilization by autoclaving. The temperature variations in the hood were kept within 2 °C during the half a day preparation. All these conditions enabled statistical compensation for barometric and temperature fluctuations, likely to influence atmospheric paramagnetic O_2 dissolution, as well as for any contamination from the material, the batches, or the atmosphere. Immediately after preparation of one sample, two NMR tubes – one duplicate was needed in case of breakage and for subsequent chemical analysis – were precisely filled with a 1-ml aliquot, and flame-sealed in less than 10 s outside the hood. The tubes of set 1 were code-labelled. All tubes of sets 1 and 2 were randomized before NMR measurements. On an average, NMR measuring generally took place within one and three weeks after preparation of the samples.

Set 1. Silica–lactose in glassware. Insoluble solid silica dioxide (Merck) was first homogenized by two successive 10 min centesimal triturations with solid lactose (1/99 w/w, Pharmadose). Two hundred milligrams of the powder obtained (corresponding to C2) were added to 20 ml of water (Biosedra for i.v. preparation) under vortex agitation. This initial liquid solution (C3) was then successively diluted, 18 times, under vortex agitation to the hundreth by addition of 0.2 ml to 19.8 ml of water in a 30 ml glass vial, using a calibrated glass dropper. The same dropper was used to fill the NMR tube and to prepare the next dilution, then was discarded. Six centesimal dilutions were retained: C6–C9–C12–C15–C18–C21 (SL-W samples). The first retained (C6) dilution contained $1.67.10^{-11}$ M silica and $2.92.10^{-8}$ M lactose. The same sequence was repeated using saline (0.15 M NaCl, Biosedra for i.v. preparation) as solvent (SL-Sal samples). Water and saline from the same batches, as controls, were similarly treated by 21 cycles of dilution/agitation (W and Sal samples). Five independent series were submitted to the same procedure.

Set 2. Silica–lactose in LiCl and polyethylene. After two successive triturations of solid silica with lactose (1/99 w/w), 20 mg of the final powder (C2) were added to 2 ml of 0.15 M LiCl (Fluka) in a 5 ml polyethylene tube (Somater, Boulogne, France) under agitation by means of the Boiron vertical stroker, then submitted to 21 successive centesimal dilution/agitation processes, by adding 20 µl to 1.98 ml of 0.15 M LiCl in the 5 ml polyethylene tube, stoppered by a plastic cap during agitation. The LiCl media were freshly prepared for each series with new batches of water (Biosedra). All steps of sampling, as well as filling of the NMR tubes, were carried out by means of pipettes with disposable plastic tips. Seven dilutions were retained: C6–C9–C12–C15–C18–C21–C24 (SL-Li). The first retained (C6) dilution contained $1.67.10^{-11}$ M silica and $2.92.10^{-8}$ M lactose. The LiCl medium underwent identical sequences as control (Li samples). Six independent series were submitted to the same procedure. No code-labelling was applied here, but the tubes were randomized before NMR measurements.

Table 1
Mean relaxation times (±standard deviations) observed in all groups of samples and linear regression analysis between relaxation times and log(centesimal dilution). A *p*-value less than 0.05 expresses the existence of a significant linear relationship (in brackets, sign of the slope (+ or −) of the regression). N.S., non significant. In italics, nearly significant.

	Ware	T1		T2		T1/T2	
		Mean (ms)	Regr. *f*(CH)	Mean (ms)	Regr. *f*(CH)	Mean	Regr. *f*(CH)
Solvent water	Glass						
W (control)		1538 ± 61	N.S.	1336 ± 97	N.S.	1.156 ± 0.084	N.S.
SL-W		1542 ± 81	N.S.	1350 ± 89	N.S.	1.144 ± 0.089	N.S.
Solvent saline	Glass						
Sal (control)		1589 ± 61	N.S.	1356 ± 75	N.S.	1.174 ± 0.069	
SL-Sal		1563 ± 64	*p = 0.057 (+)*	1352 ± 95	N.S.	1.161 ± 0.085	p = 0.036 (+)
Range C9–C21			N.S.		N.S.		p = 0.050 (+)
Solvent LiCl	Plastic						
Li (control)		1637 ± 18	N.S.	1340 ± 36	N.S.	1.222 ± 0.030	N.S.
SL-Li		1648 ± 13	p = 0.026 (+)	1379 ± 29	p = 0.012 (−)	1.196 ± 0.030	p < 0.0005 (+)
Range C9–C24			N.S.		p = 0.003 (−)		p < 0.001 (+)
Range C12–C24			N.S.		p < 0.001 (−)		p < 0.001 (+)
Heated LiCl samples	Plastic						
Li (control)		1637 ± 22	N.S.	1395 ± 41	N.S.	1.175 ± 0.036	N.S.
SL-Li		1635 ± 18	N.S.	1418 ± 42	N.S.	1.154 ± 0.036	N.S.

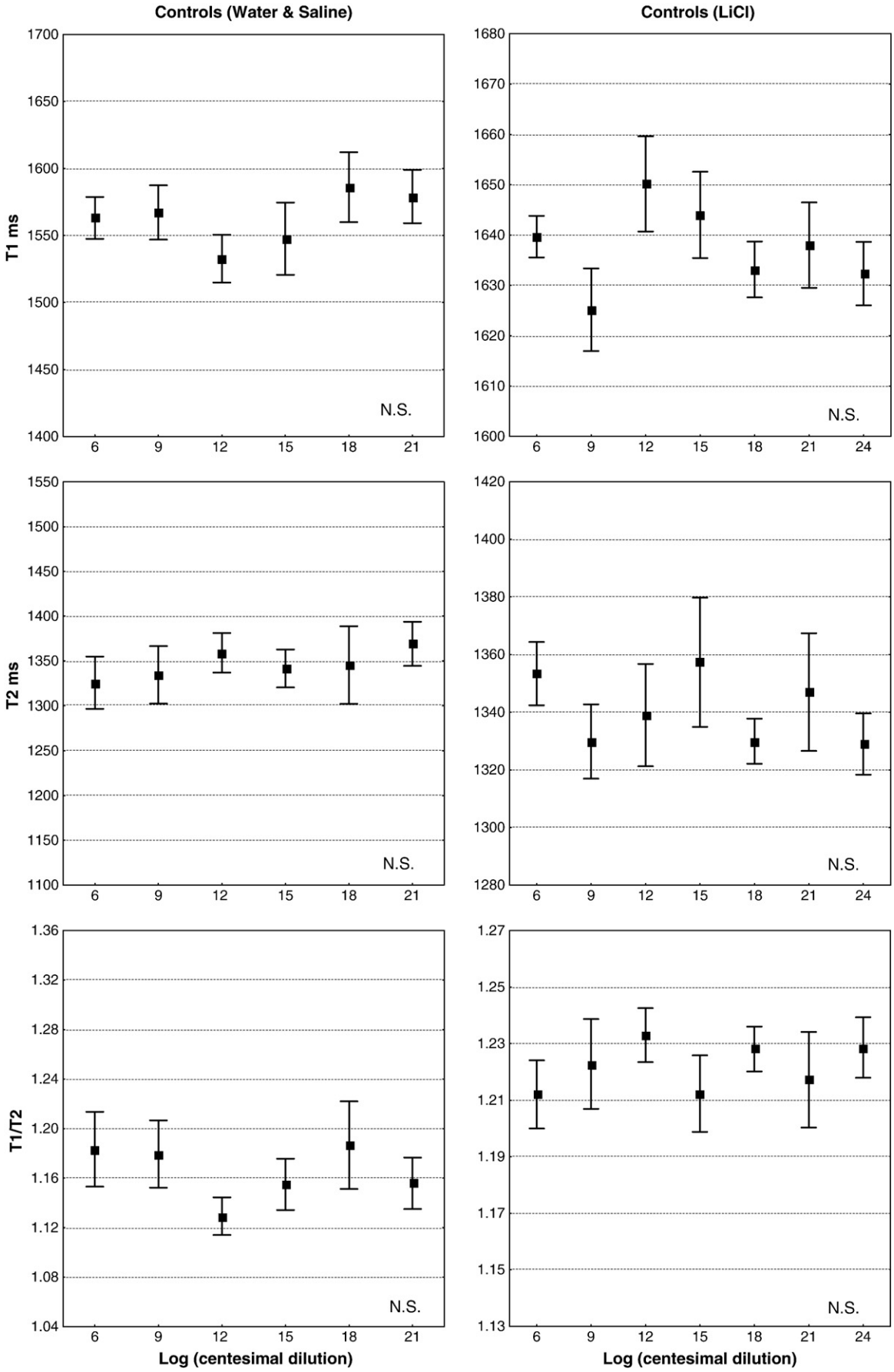

Fig. 1. Relaxation parameters T1, T2 and T1/T2 as a function of dilution in controls prepared in glassware (pooled water and saline — left) and in polyethylene (0.15 M LiCl — right). Data from the five and six series respectively are plotted with mean value and mean error. No significant variation is found as a function of dilution at the linear regression analysis.

2.2. NMR measurements

We used Bruker NMS PC 7.5 (180×7.5 mm) glass tubes. The proton relaxation times were measured at 20 MHz, on a Bruker NMS 120 Minispec. The probe temperature was maintained at 4 °C (better than ±1 °C) using a continuous circulation of non-protonated cryostatic fluid. Before any measurement, the samples were pre-cooled for 15 min in the cryostatic bath, then placed into the radiofrequency probe and allowed to reach the equilibrium temperature for at least 10 min. The longitudinal (spin–lattice) T1 and transverse (spin–spin) T2 proton relaxation time measurements were carried out using the inversion-recovery sequence (recycle delay: 20 s; real detection mode; 10 points per curve; monoexponential regression fitting) and the Carr–Purcell–Meiboom–Gill sequence (recycle delay: 20 s; magnitude detection mode; 150 points per curve; monoexponentiel regression fitting). All data were expressed in terms of relaxation time T (ms) rather than relaxivity R (ms^{-1}) for a better comparison with other published results discussed on the basis of the princeps theoretical paper of Bloembergen et al. [23].

Measurements were repeated 6 or 7 times per sample, and then averaged. After completion of measurements, the samples of set 2 were heated for 10 min in a bath of boiling deionized water, rapidly cooled, and measured again in the strictly same conditions.

2.3. Chemical analysis

At the end of the experiment, traces of silicon in the silica–lactose series were assayed by ICP on a Varian Axial atomic emission spectrometer at 251.611 nm, as described previously [20]. The assays were performed on the duplicates from one or two randomly chosen series. Given the volume required for analysis, it was necessary to pool several tubes. Glass material was imperatively excluded from these operations.

2.4. Statistical analysis

The code of the blind protocol (set 1) was only revealed when all experiments were completed. The statistical tests were performed with the Statistica (Statsoft) software. Conventional linear regression analysis, t-test for independent samples and t-paired test were used, with a significance level (p-value) set to 0.05.

3. Results

3.1. Water proton relaxation dependence on the level of dilution

Overall mean relaxation time values for controls and Sil/Lac dilutions, as well as their dependence as a function of dilution, are presented in Table 1 and Figs. 1 and 2. No consistent conclusion emerged from the comparison of the mean relaxation times between Sil/Lac solutions and their various controls, except a 2- to 3-fold larger standard deviation in samples prepared in glass material, and a higher T2 in SL-Li compared to Li controls (delta T2 = 39 ms; $p<0.0001$). By contrast, despite the large scatter of the data, some coherent behaviours could be distinguished among the different systems, statistically described by a log-linear regression $T=f$[log (centesimal dilution)], as already discussed in our previous papers [20,21]. The results of this regression analysis are summarized in Table 1. No obvious variation in relaxation times was observed in the controls in the course of the dilution/agitation process (Fig. 1), whereas significant variations occurred in the solutions (Fig. 2). Sil/Lac in LiCl exhibited the more pronounced variations with increasing dilution, i.e. a progressive increase in T1 ($p=0.026$) and a progressive decrease in T2 ($p=0.012$), resulting in a strong increase in the T1/T2 ratio ($p<0.0005$). Strikingly, these variations did persist in the very high C9–C24 and C12–C24 ranges of dilution. The difference of behaviour between Sil/Lac dilutions and controls was highlighted by means of a cross-correlation analysis (Table 2 and Fig. 3, upper row) showing that T1 and T2 are correlated positively in the controls, and negatively in the SL-Li dilutions; this was observed up to the C9–C24 and C12–C24 ranges.

For Sil/Lac in saline, similar variations were observed, nearly significant for T1 ($p=0.057$; Table 1, Fig. 2) and only as a trend for T2 (Fig. 2), probably due to the larger scatter of values; but the T1/T2 ratio increased significantly ($p=0.036$), and its slope as a function of dilution remained significant up to the C9–C21 range. Sil/Lac in water (not represented) exhibited trends similar to SL-Sal, but without significant increase in the T1/T2 ratio. However, a very significant correlation was found between the relaxation times of Sil/Lac in water and those of Sil/Lac in saline for the same dilution levels ($p=0.001$), which did persist in the C9–C21 and C12–C21 ranges (Table 3 and Fig. 4). Such a correlation was absent between pure water and saline. This noteworthy observation suggests that the presence of Sil/Lac affects the relaxation of water and saline in a similar manner, and that this modification remains detectable in the ultrahigh range of dilution.

3.2. Effect of heating

All the significant variations observed as a function of dilution in native SL-Li samples totally vanished after a 10 min heating/cooling cycle in an ebullient water bath (Table 1 and Fig. 2), and the cross-correlation analysis demonstrated the reversal of the T1/T2 ratio behaviour (Table 2 and Fig. 3, bottom row). Note that the heating/cooling cycle was directly applied on the sealed NMR tubes, thus preserving their chemical composition and gas content. Significant differences could be observed after heating, roughly similar in solutions and in controls: T1 was decreased ($p=0.001$ at the t-paired comparison test), except for the control LiCl, T2 was increased ($p<0.001$) and T1/T2 was markedly decreased ($p=0.0001$). Moreover the differences in T1 between SL-Li and Li were abolished, and those in T2 significantly reduced (delta T2: 39 to 23 ms).

3.3. Chemical analysis

High amounts of silicon (about 15–20 ppm) were found in the samples prepared in glassware (Table 4), reflecting the silica leaching from the glass, with an unexplained excess in the dilutions of silica–lactose, compared to the controls, which persisted beyond the C15 level. On the contrary, the rate of silicon was low (about 2–3 ppm) when the solutions were prepared in polyethylene material, and no excess was found in the Sil/Lac solutions when compared to the solvents.

4. Discussion

This study reports modifications of 20 MHz NMR water proton relaxation in highly diluted silica–lactose solutions in various aqueous media (water, 0.15 M NaCl, 0.15 M LiCl), at dilution levels higher than C6 (10^{-12}), i.e. far beyond the sensitivity of NMR relaxation towards magnetic or paramagnetic solutes, thus allowing to eliminate signals

Fig. 2. Relaxation parameters T1, T2 and T1/T2 as a function of dilution for silica–lactose in saline prepared in glassware (left) and for silica–lactose in 0.15 M LiCl prepared in polyethylene (right). The insets correspond to heated samples. Data from the five and six series respectively are plotted with mean value and mean error, and fitted by a linear regression function (solid line: significant $p<0.05$; dotted line: trend or nearly significant).

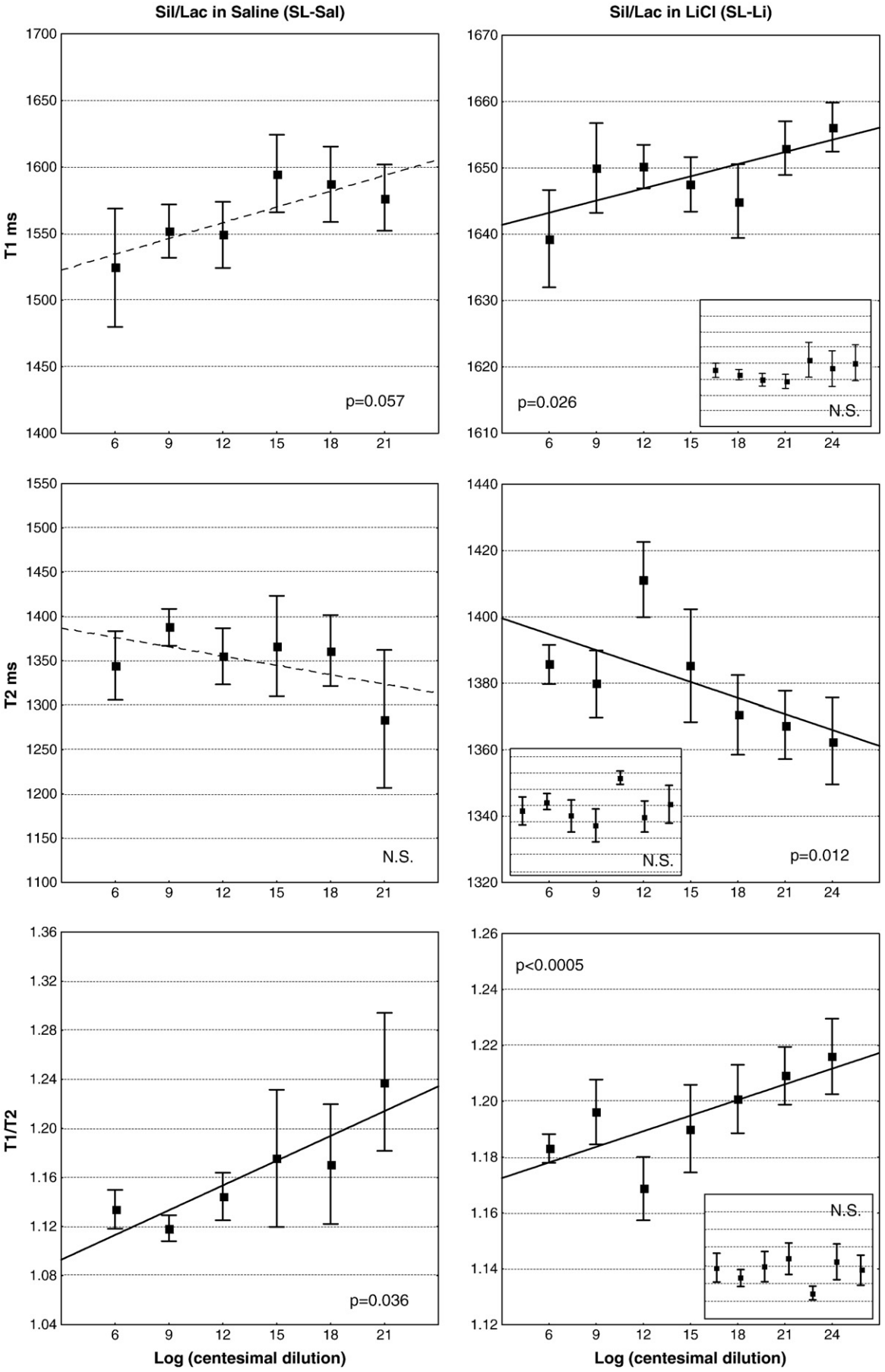
Sil/Lac in Saline (SL-Sal)
Sil/Lac in LiCl (SL-Li)
T1 ms
T2 ms
T1/T2
p=0.057
p=0.026
N.S.
N.S.
N.S.
p=0.012
p=0.036
p<0.0005
N.S.
Log (centesimal dilution)
Log (centesimal dilution)

Table 2
Linear cross-correlation analysis between relaxation parameters in Li controls and in SL-Li dilutions. The analysis compares the relaxation times at the same level of dilution. In brackets, sign (+ or −) of the slope of the regression. N.S., non significant ($p>0.05$). In italics, nearly significant. See also Fig. 3 for illustration.

	Dilution range		
	C6–C24	C9–C24	C12–C24
Controls (Li)			
T1 = *f* (T2)	$p=0.006$ (+)	$p=0.004$ (+)	$p<0.001$ (+)
T1/T2 native = *f* (T1/T2 heated)	$p<0.001$ (+)	$p<0.001$ (+)	$p<0.0001$ (+)
Dilutions (SL-Li)			
T1 = *f* (T2)	*$p=0.057$ (−)*	$p=0.029$ (−)	$p=0.042$ (−)
T1/T2 native = *f* (T1/T2 heated)	$p<0.001$ (−)	$p<0.001$ (−)	$p=0.004$ (−)

Table 3
Linear cross-correlation analysis between relaxation times in controls (water versus saline) and in Sil/Lac dilutions (water versus saline). The analysis compares the relaxation times at the same level of dilution. In brackets, sign (+ or −) of the slope of the regression. N.S., non significant ($p>0.05$). See also Fig. 4 for illustration.

	Dilution range		
	C6–C21	C9–C21	C12–C21
Water versus saline			
T1(W) = *f* [T1(Sal)]	N.S.	N.S.	N.S.
T2(W) = *f* [T2(Sal)]	N.S.	N.S.	N.S.
T1/T2(W) = *f* [T1/T2(Sal)]	N.S.	N.S.	N.S.
Sil/Lac in Water versus Sil/Lac in saline			
T1(SL-W) = *f* [T1(SL-Sal)]	$p=0.001$ (+)	$p=0.001$ (+)	$p=0.004$ (+)
T2(SL-W) = *f* [T2(SL-Sal)]	$p=0.001$ (+)	$p=0.002$ (+)	$p=0.004$ (+)
T1/T2(SL-W) = *f* [T1/T2(SL-Sal)]	$p<0.001$ (+)	$p<0.001$ (+)	$p=0.001$ (+)

coming from the solute or from its possible contaminants. This strongly suggests chemicophysical changes induced in the solvent during the specific mechanical process of dilution/agitation.

i) No modification in water proton relaxation was observed in the solvents submitted to strictly similar and simultaneous mechanical procedures.
ii) A progressive increase in T1 and decrease in T2 was observed upon dilution, more pronounced in ionic media than in water. As a result, the T1/T2 ratio exhibited a marked increase with increasing dilution in saline and especially in LiCl, where it was distinguishable up to the C12–C24 range, i.e. beyond the theoretical limit of molecular presence of solute. In water the effect was less visible, albeit a strong correlation was found between relaxation times of Sil/Lac in water and Sil/Lac in saline, which supported similar behaviours. Overall, the observed variations were dependent on the medium, following the order LiCl>NaCl>Water. The increase in T1 corroborates the decrease in relaxivity (R1 = 1/T1) reported in our 0.02–4 MHz longitudinal NMRD study on silica–lactose [20], and further reproduced with histamine at 20 MHz [21]. In both

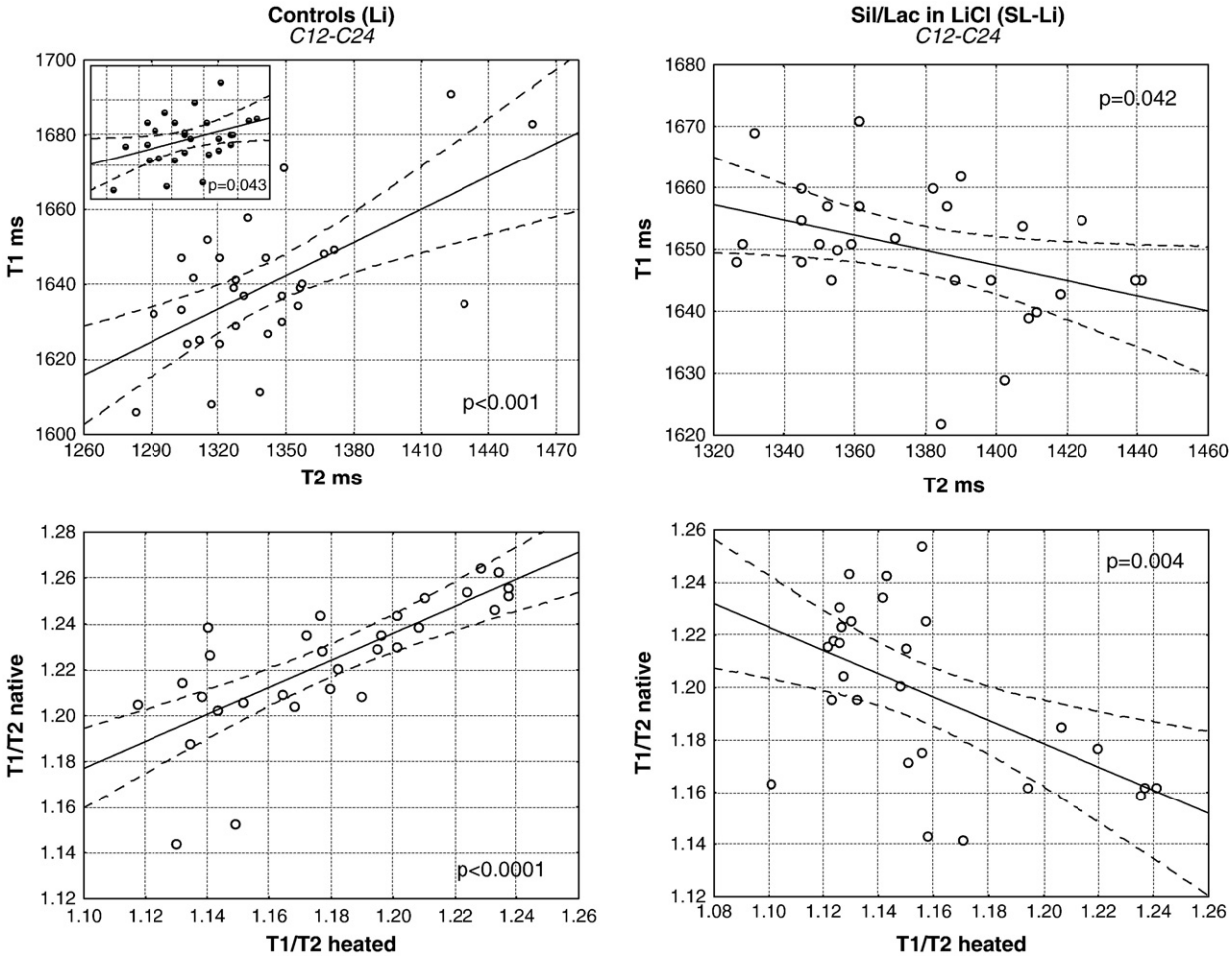

Fig. 3. Linear cross-correlation analysis in controls and in SL-Li dilutions in the ultramolecular C12–C24 dilution range. Regression lines are plotted with their 95% confidence limits (broken lines). Left: "positive correlation" in controls between T1 and T2 and between T1/T2 before heating and after heating. The inset corresponds to the analysis after exclusion of outliers. Right: "Negative correlation" between the same parameters in Sil/Lac dilutions.

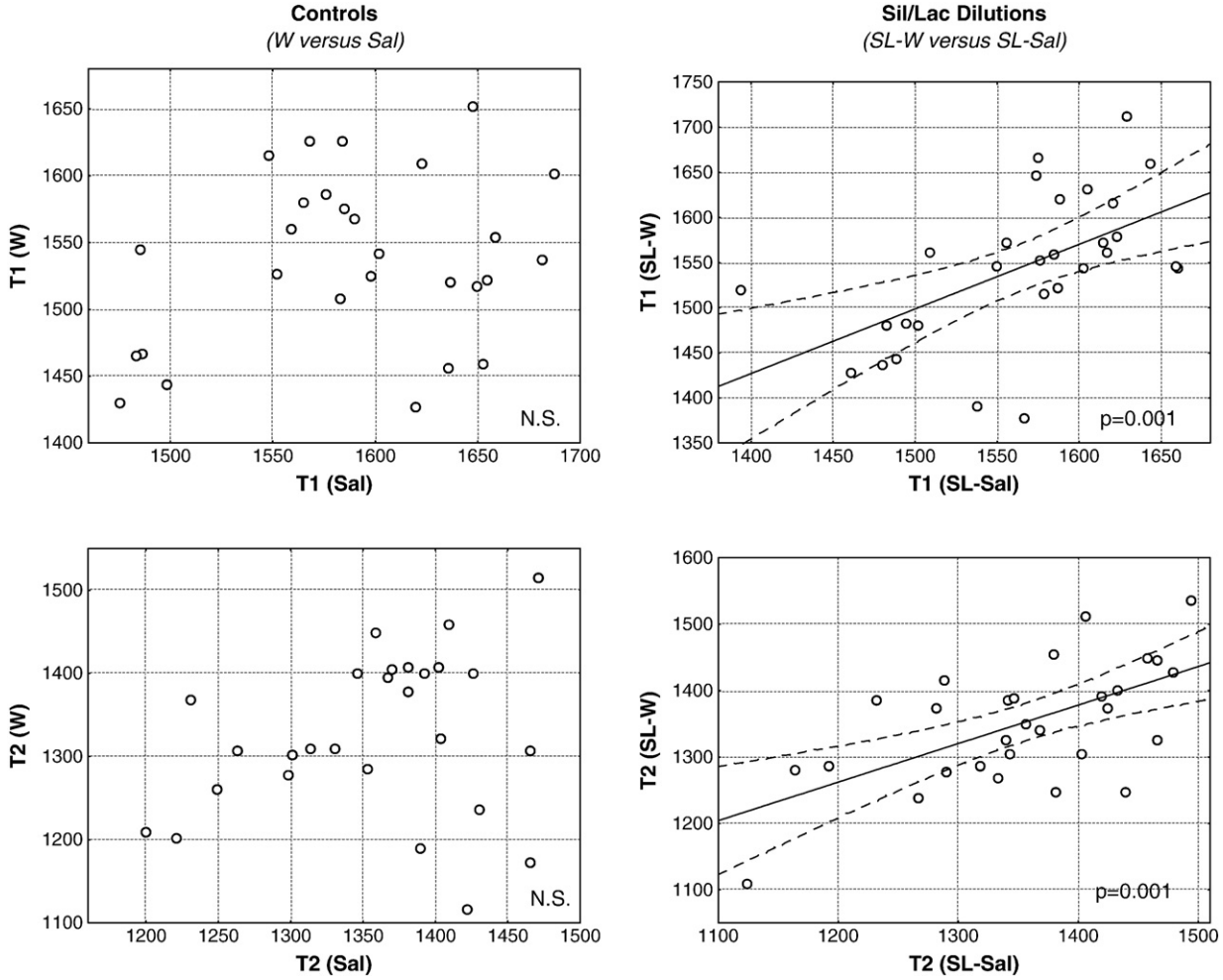

Fig. 4. Linear cross-correlation analysis of T1 and T2. Regression lines are plotted with their 95% confidence limits (broken lines). Left: controls (W versus Sal). No correlation is found between T1 in water and T1 in saline, and between T2 in water and T2 in saline. Right: Sil/Lac dilutions (SL-W versus SL-Sal). A strong correlation is observed suggesting a similar modification of the structure of water induced by the solute in the two solvents.

previous studies, the effect was more pronounced in saline than in water.

iii) The modifications in T1 and T2 observed in the SL-Li native solutions as a function of dilution totally vanished after a 10 min heating of the sealed NMR tubes, as already reported for R1 in unheated and heated dilutions of histamine [21]. Moreover, the cross-correlation analysis managed to prove the reversal of the behaviour of the T1/T2 ratio after heating. The T1/T2 ratio dropped after heating, indicating a loss of ordered structure.

iv) The previously reported NMR modifications in high dilutions prepared in glassware [18–21] were reproduced here in glassware and in polyethylene as well (where they appear to be even more pronounced due to the LiCl medium). This weakens – and even denies – the involvement of contaminating silica in the observed NMR modifications.

Table 4
Silicon content in controls and silica/lactose dilutions.

Ware	Samples	Silicon content (ppm)
Glass	Pooled (6–9–12–15–18-21 C) saline controls	15.2
	Pooled (6–9–12 C) Sil/Lac dilutions in saline	21.5
	Pooled (15–18–21 C) Sil/Lac dilutions in saline	19.0
Glass	Pooled (15–18–21 C) water and saline controls	16.5
	Pooled (15–18–21 C) Sil/Lac dilutions in water and saline	23.2
Plastic	Pooled (6-9–12–15–18–21–24 C) LiCl controls	3.1
	Pooled (6–9–12–15–18–21–24 C) Sil/Lac dilutions in LiCl	2.0

Most of these findings appear unconventional, especially the opposite behaviours of T1 and T2 in silica–lactose samples compared to the controls, these opposite behaviours persisting in the ultramolecular range, as proved by a cross-correlation analysis (Fig. 3). In pure water, for an isotropic molecular movement that can be described by a unique correlation time τ (this is the case of liquid water where rotation and translation are strongly coupled) [23]:

$$1/T1 = C\left[2\tau/\left(1+\omega_o^2\tau^2\right) + 8\tau/\left(1+4\omega_o^2\tau^2\right)\right]$$
$$1/T2 = C\left[3\tau + 5\tau/\left(1+\omega_o^2\tau^2\right) + 2\tau/\left(1+4\omega_o^2\tau^2\right)\right]$$

where $\omega_o = 2\pi.f$, f the Larmor frequency (20 MHz) (see Fig. 5A). For very short values of τ, of the order of $2.5.10^{-12}$ s in liquid state at room temperature, T1 and T2 are equal. By decreasing the temperature or introducing a solute (what induces organization and reduced mobility of the water molecules), τ progressively increases, and, as long as $\omega_o\tau \ll 1$, T1 and T2 both decrease, but T2 a little more rapidly. In that domain, T1 and T2 are "positively" correlated, as they exhibit a similar parallel variation (what is observed here in the controls). For longer correlation times ($\omega_o\tau > 1$), as those existing in ice or in concentrated systems such as tissues or macromolecular solutions

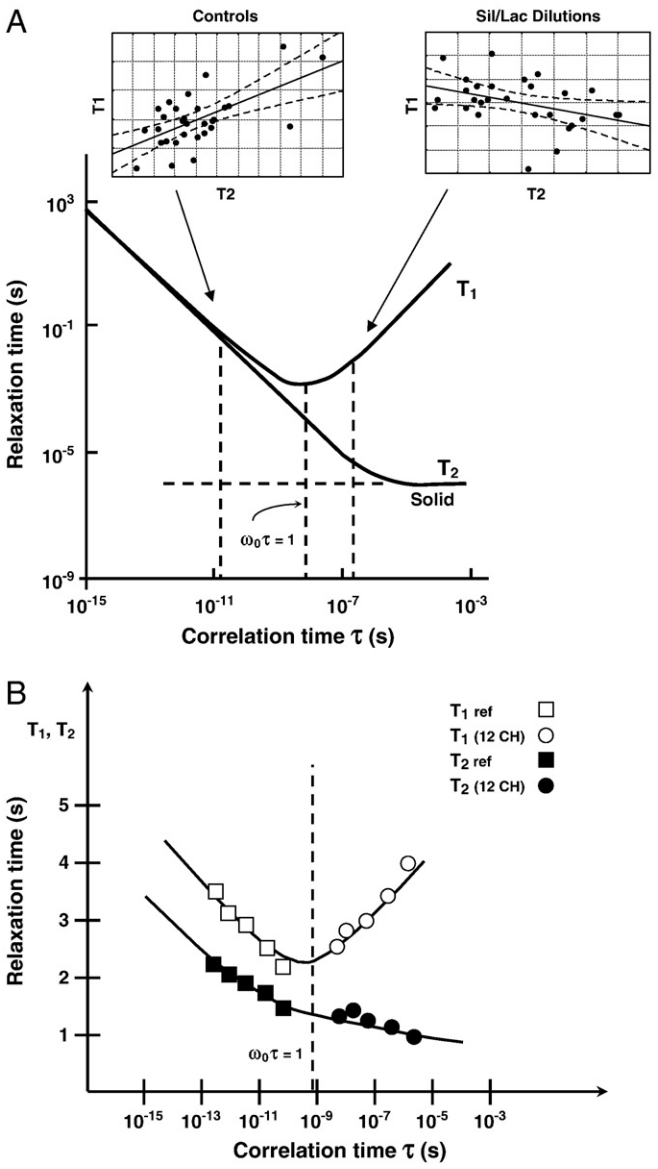

Fig. 5. (partly reprinted from Tiezzi [24] with permission): (A) Theoretical behaviour of T1 and T2 at 29 MHz for protons in water as a function of the correlation time. In our experiments carried out at 20 MHz, the minimum of T1 is very slightly shifted to the right. (B) Experimental values obtained by Tiezzi at 200 MHz for ultrahigh C12 dilutions and controls (ref). Unfortunately, neither the nature of the solutions, nor the experimental procedure were given by the author. The insets, reproduced from Fig. 3, locate the behaviours of controls and of ultramolecular Sil/Lac dilutions on the theoretical curve.

(where bound water is "frozen or icelike"), T1 and T2 start to diverge and T1 increases again, with, as a consequence, a "negative" correlation between T1 and T2 and a marked increase in the T1/T2 ratio (what is observed here for SL-Li upon dilution). A loss of correlation is thus expected in the transitional region (minimum of the curve), where the correlation times of the water molecules reach 5.10^{-9} s at 20 MHz. As the rotational correlation time is given by $\tau = 4\pi\eta a^3/3kT$, the increase in τ reflects either a viscosity change (η term) or, more probably, a change in the radius (a term) of the water domain visited by the proton during resonance. For $\tau = 5.10^{-9}$ s, the calculation leads to a radius of 2.1 nm, what allows us to postulate the presence of larger than 4-nm diameter supramolecular structures with collective orientational motion slower than a few hundred picoseconds. Interestingly, Tiezzi [24] reached the evidence for supramolecular structures from a similar interpretation of divergent behaviours of T1 and T2 at 200 MHz in high dilutions compared to solvent (see Fig. 5B). As already discussed in our study on histamine [21], we postulate the involvement of nanobubbles in these superstructures on account of the cancelling of the NMR signals after heating, and of NMR relaxation observations by Kondrachuk [25] reporting a structuring effect of atmospheric gases on water which disappear after boiling. Moreover, the estimated size of the superstructures seems to agree with the smallest air nanobubbles ($d = 3.6$–4.0 nm) demonstrated in water by small-angle neutron scattering [26]. Denoting by f the fraction of water engaged in the proposed superstructures, the experimental relaxation rate can be written:

$$(1/T)_{\text{exp}} = f.(1/T)_{\text{superstr.}} + (1-f).(1/T)_{\text{bulk}}$$

Owing to the negligible concentration of solute (f theoretically negligible), the experimental detection of relaxation changes necessarily implies either a cooperative process of recruiting (increasing f), or a drastic decrease in relaxation times, or both. Highly ordered superstructures do satisfy these two conditions. From the above equations, with τ lying between 10^{-9} and 10^{-8} s, one can calculate that a 2.10^{-5} fraction of highly organized water is enough to explain a 30 ms variation (likely to be detected) in the relaxation times. At normal temperature and pressure, dissolved air in water has a concentration of around 1 mM, that is a gas/water ratio of 2.10^{-5}; so, it is enough to consider the clustering of water around gases to reach this fraction.

Small nanosized bubbles (10 nm on average) have been identified in liquid water [26–29], which are stabilized by traces of ions and tend to associate in fractal clusters, that scatter light. Removal of gases suppresses the light scattering by water [30]. The gas–water interface of the nanobubbles is hydrophobic, and therefore the water molecules may form shells of hardly hydrogen-bonded, "icelike" structures, around the nanobubbles [31,32]. These ordered shells can induce long range structure up to the micrometer level [33]. Submicroscopic bubbles may arise from mechanical agitation or nucleation of dissolved air around low pressure vortexes, especially near hydrophobic rough surfaces [29,34,35]. Let us propose that the vigorous mechanical agitation used here enhances the formation of nanobubbles in the negative pressure regions and that the introduction of the solute acts as a nucleation centre, promoting polymolecular edifices, composed of water, electrolytes if any, and nanobubbles. The evidence for rather stable nanobubbles implied within the supramolecular structures formed around small organic molecules in water as demonstrated by laser light scattering supports this view [36]. The progressive increase of the T1/T2 ratio as a function of dilution shown here could suggest that the superstructures develop more upon dilution. The more pronounced effect found in salt media compared to pure water might merely reflect an enhanced "nanobubble effect", since ions stabilize nanobubbles [27] and since ionic concentrations higher than 0.1 M are known to inhibit their coalescence [37–41]. The greater effect found in LiCl compared to NaCl may result from a combination among many factors: *i)* the larger number of water molecules in the solvation shell of the Li^+ cation reported from transport number measurements [42] or from colligative properties [43], *ii)* the stronger structure making properties of the Li^+ cation demonstrated in viscosity and NMR relaxation measurements (review in [44]), *iii)* the increased residence time of water molecules in the first hydration shell [45,46], and *iv)* the quite different behaviour of Li^+ and Na^+ in silicate and polysilicate systems, especially the stabilizing effect of Li^+ [22].

Of course, other kinds of superstructures without involvement of gases can be proposed, such as large water or ion–water clusters, as there is a growing experimental evidence for water clustering, in pure water and ionic solutions, from several tens up to 200 molecules [review in [47,48]]. Noteworthy, thermal rotation of water molecules in charged $H^+(H_2O)_n$ clusters has been estimated of the order of 10^{-6} s at 25 °C [49,50] and cooperative orientational motion of water

molecules in liquid water and around solute molecules may persist more than 300 ps [51] and over very long distances (≈300 nm [52]).

This work also questioned the possible role of silica leaching from the glass. An intriguing higher amount of leached silica was found in silica–lactose samples prepared in glassware, compared to controls, even at ultrahigh levels of dilution, beyond C15. This confirms our previous finding [20] and is not yet explained. It may reflect a catalytic effect of silica when initially present in the solution. Silica exists as soluble monosilicic and polysilicic acids, and as insoluble colloidal nanoparticles, especially in supersaturated solutions. When silica is present in supersaturated solutions (as in the C3 dilution), the leached silicic acid deposits on silica particles, thus allowing more silicic acid to dissolve from the glass surface. Such a mechanism is likely strongly enhanced by the vigorous shaking procedure. In samples prepared in plastic ware, on the contrary, low amounts of silica were found (2–3 ppm), which only reflect the leaching during the storage in the NMR test tube.

Coming back to Montagnier's paper [17], our successive NMR studies since 2004 argue for the presence of nanosized superstructures in high dilutions prepared under strong agitation, which seem to develop more upon dilution and are destroyed after heating.

Acknowledgements

The work was supported by a grant from Institut Boiron, 69110 Sainte-Foy-lès-Lyon.

References

[1] J. Kleijnen, P. Knipschild, G. ter Riet, Br. Med. J. 302 (1991) 316.
[2] K. Linde, W.B. Jonas, D. Melchart, F. Worku, H. Wagner, F. Eitel, Hum. Exp. Toxicol. 13 (1994) 481.
[3] K. Linde, N. Clausius, G. Ramirez, D. Melchart, F. Eitel, L.V. Hedges, W.B. Jonas, Lancet 350 (1997) 834.
[4] M. Cucherat, M.C. Haugh, M. Gooch, J.P. Boissel, Eur. J. Pharmacol. 56 (2000) 27.
[5] A. Shang, K. Huwiler-Müntener, L. Nartey, P. Jüni, S. Dörig, J.A.C. Sterne, D. Pewsner, M. Egger, Lancet 366 (2005) 726.
[6] Editorial, Lancet 366 (2005) 690.
[7] E. Davenas, F. Beauvais, J. Amara, M. Oberbaum, B. Robinzon, A. Miadonna, A. Tedeschi, B. Pomeranz, P. Fortner, P. Belon, J. Sainte-Laudy, B. Poitevin, J. Benveniste, Nature 333 (1988) 816.
[8] Editorial, Nature 333 (1988) 787.
[9] J. Maddox, Nature 334 (1988) 287.
[10] P. Coles, Nature 334 (1988) p372.
[11] J. Aïssa, M.H. Litime, E. Attias, J. Benveniste, J. Imunol. 150 (1993) A146.
[12] J. Benveniste, J. Aïssa, M.H. Litime, G.T. Tsangaris, Y. Thomas, FASEB J. 8 (1994) A398.
[13] Y. Thomas, M. Schiff, L. Belkadi, P. Jurgens, L. Kahhak, J. Benveniste, Med. Hypotheses 54 (2000) 33.
[14] P.C. Endler, W. Pongratz, C.W. Smith, J. Schulte, Vet. Hum. Toxicol. 37 (1995) 259.
[15] F. Senekowitsch, P.C. Endler, W. Pongratz, C.W. Smith, FASEB J. 9 (1995) A12161.
[16] W.B. Jonas, J.A. Ives, F. Rollwagen, D.W. Denman, K. Hintz, M. Hammer, C. Crawford, K. Henry, FASEB J. 20 (2006) 23.
[17] L. Montagnier, J. Aïssa, S. Ferris, J.L. Montagnier, C. Lavallée, Interdiscip. Sci. Comput. Life Sci. 1 (2009) 81.
[18] J.L. Demangeat, C. Demangeat, P. Gries, B. Poitevin, A. Constantinesco, J. Med. Nucl. Biophys. 16 (1992) 135.
[19] J.L. Demangeat, P. Gries, B. Poitevin, in: M. Bastide (Ed.), Signals and Images, Kluwer Academic Publishers, Dordrecht, 1997, p. 95.
[20] J.L. Demangeat, P. Gries, B. Poitevin, J.J. Droesbeke, T. Zahaf, F. Maton, C. Piérart, R. N. Muller, Appl. Magn. Reson. 26 (2004) 465.
[21] J.L. Demangeat, J. Mol. Liq. 144 (2009) 32.
[22] R.K. Iler, in: R.K. Iler (Ed.), The Chemistry of Silica, Wyley, New York, 1979, p. 3, (chapt 1–4).
[23] N. Bloembergen, E.M. Purcell, R.V. Pound, Phys. Rev. 73 (1948) 679.
[24] E. Tiezzi, Ann. Chim. 93 (2003) 471.
[25] A.V. Kondrachuk, V.V. Krasnogolovets, A.I. Ovcharenko, E.D. Chesnokov, Sov. J. Chem. Phys. 12 (1994) 1485.
[26] N.F. Bunkin, A.V. Lobeyev, O.I. Vinogradova, T.G. Movchan, A.I. Kuklin, JETP Lett. 62 (1995) 685.
[27] N.F. Bunkin, F.W. Bunkin, Sov. Phys. JETP 74 (1992) 271.
[28] N.F. Bunkin, A.V. Lobeyev, JETP Lett. 58 (1993) 94.
[29] O.I. Vinogradova, N.F. Bunkin, N.V. Churaev, O.A. Kiseleva, A.V. Lobeyev, B.W. Ninham, J. Colloid Interface Sci. 173 (1995) 443.
[30] N.F. Bunkin, A.V. Lobeyev, Phys. Lett. A 229 (1997) 327.
[31] M. Colic, D. Morse, Phys. Rev. Lett. 80 (1998) 2465.
[32] K. Ohgaki, N.Q. Khanh, Y. Joden, A. Tsuji, T. Nakagawa, Chem. Eng. Sci. 65 (2010) 1296.
[33] Y. Katsir, L. Miller, Y. Aharonov, E.B. Jacob, J. Electrochem. Soc. 154 (2007) D249.
[34] J.L. Parker, P.M. Cleasson, P. Attard, J. Phys. Chem. 98 (1994) 8468.
[35] J. Yang, J. Duan, D. Fornasiero, J. Ralston, J. Phys. Chem. B 107 (2003) 6139.
[36] F. Jin, J. Ye, L. Hong, H. Lam, C. Wu, J. Phys. Chem. B 111 (2007) 2255.
[37] R.R. Lessard, S.A. Zieminski, Ind. Eng. Chem. Fundam. 10 (1971) 260.
[38] V.S.J. Craig, B.W. Ninham, R.M. Paschley, J. Phys. Chem. 97 (1993) 10192.
[39] U. Hofmeier, V.V. Yaminsky, H.K. Christenson, J. Colloid Interface Sci. 174 (1995) 199.
[40] P.K. Weissenborn, R.J. Pugh, J. Colloid Interface Sci. 184 (1996) 550.
[41] V.S.J. Craig, Curr. Opin. Colloid Interface Sci. 9 (2004) 178.
[42] C.H. Hamann, W. Vielstich, Elektrochemie, 3rd ed., Wiley, Weinheim, 1998, p. 25.
[43] A.A. Zavitsas, J. Phys. Chem. B 105 (2001) 7805.
[44] Y. Marcus, Chem. Rev. 109 (2009) 1346.
[45] R.W. Impey, P.A. Madden, I.R. Mc Donald, J. Phys. Chem. 87 (1983) 5071.
[46] U. Kaatze, J. Solut. Chem. 26 (1997) 1049.
[47] M.F. Chaplin, Biophys. Chem. 83 (1999) 211.
[48] T.H. Plumridge, R.D. Waigh, J. Pharmacy, Pharmacology 54 (2002) 1155.
[49] B.E. Conway, J.O'.M. Bockris, H. Linton, J. Chem. Phys. 24 (1956) 834.
[50] P.M. Holland, A.W. Castleman, J. Chem. Phys. 72 (1980) 5984.
[51] J. Higo, M. Sasai, H. Shirai, H. Nakamura, T. Kugimiya, PNAS 98 (2001) 5961.
[52] D.P. Shelton, Chem. Phys. Lett. 325 (2000) 513.